Science Advances Manuscript Template

## Title

- Full title: "Touch as an auxiliary proprioceptive cue for movement control"
- Short titles "Touch as an auxiliary proprioceptive cue"


## Authors

A. Moscatelli,[1,2*†] M. Bianchi[3*†], S. Ciotti, [3,5] G. C. Bettelani,[3] C.V. Parise[4], F. Lacquaniti[1,2], A. Bicchi[3,5].

## Affiliations

[1]Department of Systems Medicine and Centre of Space Bio-medicine, University of Rome "Tor Vergata", Rome, Italy.
[2]Laboratory of Neuromotor Physiology, Fondazione Santa Lucia IRCCS, Rome, Italy.
[3]Centro di Ricerca "E. Piaggio" and Dipartimento Ingegneria dell'Informazione, University of Pisa, Pisa, Italy.
[4]Oculus Research, Redmond, Washington, United States of America.
[5]SoftBots Lab - Soft Robotics for Human Cooperation and Rehabilitation, Istituto Italiano di Tecnologia, IIT, Genoa, Italy

*a.moscatelli@hsantalucia.it; matteo.bianchi@centropiaggio.unipi.it

† These authors contributed equally to this work.



## Abstract

Recent studies extended the classical view that touch is mainly devoted to the perception of the external world. Perceptual tasks where the hand was stationary demonstrated that cutaneous stimuli from contact with objects provide the illusion of hand displacement. Here, we tested the hypothesis that touch provides auxiliary proprioceptive feedback for guiding actions. We used a well-established perceptual phenomenon to dissociate the estimates of reaching direction from touch and musculoskeletal proprioception. Participants slid their fingertip on a ridged plate to move towards a target without any visual feedback on hand location. Tactile motion estimates were biased by ridge orientation, inducing a systematic deviation in hand trajectories in accordance with our hypothesis. Results are in agreement with an ideal observer model, where motion estimates from different somatosensory cues are optimally integrated for the control of movement. These outcomes shed new light on the interplay between proprioception and touch in active tasks.


Teaser: Behavioral data and model show that cutaneous stimuli from contact with objects provide auxiliary proprioceptive feedback for guiding actions.

## MAIN TEXT

### Introduction

Mechanoreceptors embedded in the skin and in subcutaneous tissues are the mechanical sensory interface between our body and its surroundings (*1*). Afferent fibers convey the mechanical stimuli encoded by the mechanoreceptors to the central nervous system. Tactile information processed in the somatosensory areas supports both action and perception. It provides feedback to the motor system while manipulating objects, and at the same time it conveys perceptual information on the object itself, such as its texture, softness, weight, and motion status (*2*, *3*). This function of touch, the perception of the external world as it impacts on the body, is known as exteroception (*1*).

Although exteroception has often been regarded as the main function of touch, recent studies have demonstrated that cutaneous signals can also provide cues for proprioception (the sense of position and movement of our limbs and trunk) in perceptual tasks. (*4*). For example, in addition to contact with objects, mechanoreceptors respond to the skin strain associated with flexion-extension of the joints, and therefore touch can inform our brain about body posture and the location of our limbs in space (*4*, *5*). The deformation of the skin from the interaction with objects influences perceptual judgements about hand position and displacement. In tasks involving passive touch, where the hand is either stationary or passively displaced, specific cutaneous stimuli arising from the contact of objects with our body, as for example the rotational motion of a surface on the palm, or a change in contact area while pushing on a soft interface, provide the illusory sensation of hand displacement (*6*–*8*). This is defined as extrasomatic information because—unlike the other proprioceptive signals, such as those arising from muscle spindles, Golgi tendon organs or joint receptors—it is generated by the contact with external objects (*8*). The use of cutaneous signals as auxiliary proprioceptive cues leverages upon knowledge or assumptions about the objects being touched. For example, an observer may assume that material properties like the softness or granularity of the surface are constant, and that inanimate objects are stationary (*8*, *9*). Given these assumptions, a deformation on the skin is more likely to be interpreted as our limbs hitting against a static object rather than a moving object impacting on our static limbs; that is, humans are more likely to move than inanimate things in the environment.

The perceptual illusions discussed above demonstrate the role of cutaneous touch as an auxiliary proprioceptive cue in passive perceptual tasks. Similarly, studies on deafferented patients highlighted the importance of somatosensory feedback for motor control (*10*). The two patients described in (*10*) presented a severe, purely sensory neuropathy, and this caused an impairment in performing daily-life actions, including object grasping and manipulation. Taken together, these studies suggest the intriguing hypothesis that cutaneous touch may provide auxiliary information for the control of hand movement. We evaluated this in dynamic reaching tasks, where participants slid their finger on a surface along a target direction. It is far from obvious that the findings from perceptual tasks will apply to motor control: Neuropsychological literature and perceptual illusions offer several examples of dissociation between perception and action (*11*–*13*). For instance, vibrating the biceps tendons creates the illusory sensation of arm displacement in passive perceptual tasks. However, the same participants could accurately reach for the vibrating arm with the other arm, thereby demonstrating that the motor system was less prone to this illusion (*12*). This might be due to the contribution of endogenous signals from motor areas, which provide redundant cues for limb position in reaching tasks, thereby increasing the robustness of the motion estimate. Indeed, the control of movement is based on forward models of the motor command—referred to as the efference copy—that specifies the predicted position of the hand during voluntary actions (*14*, *15*). In the example in (*12*), the biased sensory signal from tendon vibration may produce a smaller effect in the reaching task because the estimate of the hand position is partially corrected by the efference copy. Besides that, dissociations between perception and action have been explained by postulating the existence of two independent representations of the body, the body schema for motor control and the body image for conscious perception (*12*). The former would provide the sensorimotor system with an implicit representation of the body, used for the control of movement. Instead, information on limb position and displacement would affect the body image in perceptual tasks, such as in tasks requiring the overt identification of a body part (*10*, *12*), and perceptual judgements on limb displacement and motion (*6*–*8*). In the current study, we tested hypothesis that, unlike tendon vibration, auxiliary proprioceptive cues from contact with objects would produce an effect also on the body schema, hence affecting motor control in active tasks.

A major challenge to measure the contribution of touch in guiding reaching actions is to dissociate it from the other redundant somatosensory cues from the musculoskeletal system. Here, we used a well-established tactile phenomenon to decouple the two motion estimates. Previous studies on passive touch, in which participants kept the hand world-stationary while the underlying surface moved, showed that the perceived motion direction of a surface with parallel raised ridges was strongly biased towards the axis perpendicular to the ridges (*16*, *17*). This arises from the fact that, neglecting friction (e.g., for a lubricated surface), motion parallel to the ridges does not produce relevant changes in tissue strain (*16*). We used this phenomenon to parametrically dissociate tactile from other somatosensory cues in active hand motion. In a series of three experiments, we asked blindfolded participants to slide their finger on a static surface with parallel raised ridges, trying to move the hand along a straight direction away from their body (Exp. 1-2) or to reach for a visual target displayed through a Head Mounted Display (Exp. 3). The orientation of the ridges varied across trials. If touch operates as an auxiliary proprioceptive cue, the orientation of the ridges should produce a systematic error in hand trajectory, because the observer would take into account the biased tactile signal to estimate motion direction.

As previous studies have demonstrated, human behavior is well accounted for by models of motor control where redundant sensory cues are dynamically integrated and compared to the efference copy, to provide the optimal estimate of the state of the system (*14*, *15*, *18*, *19*). Therefore, if touch is indeed an auxiliary cue for proprioception, it would be reasonable to hypothesize that cutaneous and extracutaneous information on hand motion should be dynamically integrated in our reaching tasks. To test this corollary hypothesis, we developed an ideal observer model based on Kalman filtering, and we compared its prediction to our empirical findings. Models of optimal integration, including dynamic models, predict that the contribution of each sensory channel to the fused estimate depends on its reliability (*20*). This leads to the counterintuitive prediction that in our task participants with a tactile input made unreliable by wearing a glove will be more accurate in reaching for the target direction. We found that cutaneous information systematically biases reaching movements and the results are in line with the prediction of the Kalman filter, thereby demonstrating that cutaneous touch is indeed an auxiliary cue for proprioception.

## Results

**Experiment 1: Hand Reaching.** In a first experiment, we asked blindfolded participants (n = 10) to slide their finger on a static surface with parallel ridges, trying to move the hand straight away, along their body mid-line (Fig. 1). Participants were required to move along the goal direction with a slow self-paced hand movement, and to stop before reaching the farther edge of the plate. Before each trial, a servomotor rotated the contact surface to change the orientation of the ridges. If reaching movements were accurate, participants should follow a direction straight away from them, illustrated by the solid arrow in Fig. 1B. Instead, if our hypothesis is true and the sensory feedback to motor control included the tactile signal, we expect a systematic error in hand trajectory depending on the orientation of the ridges (Fig. 1 B–C).

[Fig. 1 about here]

To test this hypothesis, we computed the motion angle in each trial and evaluated its relationship with the orientation of the ridges. Negative motion angles indicate that the hand trajectory rotated clockwise with respect to the solid arrow in Fig. 1B, and *vice versa* (see Fig S1 in Supplemental Data). We fit the data with the Linear Mixed Model in Eq. 1 that takes into account the effect of the experimental variables (fixed-effect parameter), the variability between participants (random-effect parameter), and the residual error. In particular, the fixed-effect slope of the linear model, labelled as $\beta_1$ in the equation, estimated the effect of the orientation of the ridges on the motion angle. In accordance with our hypothesis, the motion angle changed with the orientation of the ridges (effect size: $-0.15 \pm 0.03$, $\beta_1 \pm$ Std. Error). In other terms, a clockwise rotation of the ridges with respect to the frontal plane caused the participants to deviate hand motion from straight by bending leftwards, and *vice versa*. This effect was statistically significant ($\chi_1$ = 13.0, p = 0.0003). The linear dependency between the motion angle and the orientation of the ridges is illustrated in Fig. 2A in a representative participant and in Fig. 2B in the whole population. By inspecting the individual trials in Fig 1C, we can see that the trajectory deviated nearly immediately from the target goal direction because the finger was in contact with a raised ridge at the trial onset. The ideal observer model illustrated in model section predicts this behavior. The linear function in Fig 2A has a small offset, leading to a larger absolute motor bias with clockwise-rotated stimuli. This offset was possibly due to extra-cutaneous signals. To verify this hypothesis, we replicated the task with a smooth plate. In the absence of the oriented texture, any systematic deviation from zero in the motion angle would arise from extra-cutaneous signals. We estimated the systematic error in motion angle from Eq. 2, which was equal to $4.2 \pm 1.925$ deg ($\beta_0^* \pm$ Std. Error). Correcting for this additional motor bias, the offset in model was non-significantly different from zero, that is, the motion angle was symmetric between clockwise- and counterclockwise-rotated stimuli.

It is worth noting that participants were not following the ridges. If this were the case, the absolute error would have been larger for $\pm 30°$ stimuli and smaller for $\pm 60°$, which was the opposite of what we found. This is further explained in Supplementary Figure S6. Next, we analyzed the force data to test whether contact force modulated the relationship between motion angle and ridge orientation. The median value of peak force was 0.89 N (95% percentile range from 0.04 to 1.87 N; see Supplemental Data). The analysis of the force data confirmed a significant effect of ridge orientation also when including the contact force as predictor ($\chi_1 = 4.6$, $p = 0.031$; see Supplemental Data). Neither the effect of contact force nor its interaction with ridge orientation were statistically significant. To evaluate the role of frictional forces on hand trajectory, four participants replicated the experiment using a lubricated surface (Exp. 1b). Results of Experiment 1b confirmed the relationship between the ridge orientation and the motion angle (effect size: $-0.25 \pm 0.08$, $\beta_1 \pm$ Std. Error), thus ruling out any effect of frictional forces on the observed phenomenon. The effect of ridges was still statistically significant ($\chi_1 = 4.68$, $p = 0.03$).

[Fig. 2 about here]

**Experiment 2: Angular error and reliability of the tactile signal.** Results of Exp. 1 supported the hypothesis of the integration between somatosensory cues for the estimate of reaching direction. Models of optimal integration predict that the weight of each sensory cue in the fused estimate depends on its reliability, with the reliability of each signal being the inverse of its variance (*20*). In a second experiment we tested the hypothesis of the optimal integration by asking participants (n = 11) to replicate the same task, either with their bare fingertip as in Exp. 1, or by wearing a rubber glove that is known to reduce the reliability of the tactile signal (*21*). Under the assumption of optimal integration, the effect of ridge orientation should be weaker when performing the task while wearing the glove, because this reduced the weight of the tactile channel in the fused estimate. That is, the contribution of touch to the integrated motion estimated should be smaller. We analyzed the data with the LMM in Eq. 3 including ridge orientation, the presence of the glove, and the interaction of the two as fixed-effect predictors. Without the glove, we found a similar effect to the one found in Exp. 1, that is, hand trajectory deviated towards a direction parallel to the ridges ($\eta_1 = -0.16 \pm 0.04$). Crucially, the presence of the glove reduced the effect size, and the interaction between ridges and glove was statistically significant ($\eta_2 = 0.11 \pm 0.04$). As illustrated in Fig. 2C-D, the slope of the linear relationship between the motion angle and the ridges was significantly more negative without the glove than with it ($\chi_1$= 5.3, p = 0.02), in accordance with our hypothesis. The estimated slope changed from $-0.16$ without glove to $-0.05$ with glove. We confirmed this result with a bootstrap method, as explained in (*22*). The 95% confidence interval (CI) of the interaction term $\eta_2$ did not include zero, with the inferior and the superior CI equal to 0.03 and 0.19, respectively. Peak force was slightly larger in the condition with glove compared to bare fingertip ($p < 0.001$). Without glove, the average value of force peak for a perpendicular (zero) orientation of the stimulus was equal to $0.62 \pm 0.07$ N, and increased slightly with glove (the difference between the conditions was equal to $0.25 \pm 0.08$ N). This small increase in contact force when wearing a glove is in accordance with literature on grasping forces in lifting and holding tasks (*23*). To further support our main result from Exp. 1, i.e., that ridge orientation produced a bias in the reaching trajectory, we additionally tested 10 naïve participants without glove (five plate orientation, ten repetitions each, as in Exp. 2). Combining the new sample and the "without glove" condition lead to a sample size of twenty-one participants performing the task with the bare finger. The effect of ridge orientation was highly significant ($\chi_1 = 17.5$, $p < 0.0001$), which confirmed our findings in Exp. 1.

**Experiment 3: Reaching towards visual targets.** In a third experiment (n = 8), we extended the results of Exp. 1-2 to a more immersive task, requiring participants to reach for a visual target displayed with a Head Mounted Display (HMD). Differently from the repetitive movement in the first two experiments, the third experiment prompted participants to change their motor plan between trials, enhancing the role of the efference copy in the task. Our hypothesis implies the dynamic integration of both, endogenous and sensory signals (as formalized in model section); if so, we should still observe a dependency on ridge orientation for the three different targets. The virtual scene consisted of a circular plate without ridges, having the same size and position in space as the real plate (Fig. 3A). At the trial onset, the experimenter placed the finger of the participant on the real plate on the starting point. Thereafter, a visual target consisting of a sphere of one cm radius briefly flashed on the virtual plate. The visual target was placed on the arc of an ideal circumference with radius of 5 cm, in one of the following angular position: $-15°$, $0°$, $15°$ (Fig. 3A). Participants were instructed to slide the hand over the textured plate to reach for the target. Prior to each trial, the plate was rotated by the motor to one of the following angular position: $-60°$, $0°$, $60°$ with respect to the virtual target. The visual stimulus did not provide any feedback on the actual hand position and motion, and on the rotation of the physical plate (Fig. 3A). This experimental protocol allowed us to manipulate independently the target position (hence, the motor goal) and the orientation of the ridges. Results of Exp. 3 supported our main finding that ridge orientation produces a systematic error in reaching (Fig. 3B-C). For all target positions, the hand trajectory deviated towards the direction of the longitudinal axis of the ridges (effect size: $-0.056 \pm 0.01$, $\theta_1 \pm$ Std. Error), in accordance with the other two experiments. The effect was statistically significant ($\chi_1$= 13.3, p = 0.0003). The difference in the intercept between the three linear functions in Fig. 3B accounts for the three target goals.

The median value of peak velocity ranged between 7 and 25 cm/s in the three experiments. This is less than the value reported in other studies—for e.g., 60 cm/s in (*24*)—because of the small workspace and because we asked participants to move slowly. See Supplemental Data for the analysis of the contact force and peak velocity in Exp. 1-3.

[Fig. 3 about here]

**Kalman Filter Model**

Observer models based on Kalman filtering have been used to describe human behavior in different motor tasks, such as those requiring hand reaching (*14*, *18*, *19*) and eye movement (*25*). Here, we introduce an observer model for the integration of proprioception and touch in motor control. The model formalizes the two hypotheses of the study, that the biased tactile signal produced a systematic error in hand trajectory, and that the strength of this phenomenon depends on the reliability of the tactile signal. We simulate the outcome of the model and show that it reproduces all patterns in the current experimental data. The model consists of two processes (Fig. 4). In the first one, a forward model predicts the following state of the hand direction based on the estimate of the current state and the motor command. The forward model corresponds to the efference copy in motor control literature (*15*). In the second process, the direction of motion is measured by the somatosensory cues. Unlike previous studies, in our model the sensory measurement arises from the optimal integration of touch and proprioception, where each of the two signals is weighted depending on its reliability. The integration of the two signals implies the assumption that the touched surface is world-stationary. If this is the case, touch and extra-cutaneous signals provide the agent with redundant information, which can be integrated for an optimal estimate of hand displacement. Next, the internal estimate is compared to the sensory measurement generating an error term. The error term, weighted by a gain factor (i.e., the Kalman gain), is then used to update the estimate of the system. Finally, a motor command is generated to correct for the difference between the updated state estimate and the goal direction.

[Fig. 4 about here]

Model equations are illustrated in Fig. 4 and in the Methods Section. Symbols used in model equations are listed in Table 1. The model has three free parameters, which are the weight of the tactile signal, $w_T$ (with the weight of the proprioceptive signal $w_P = 1 - w_T$), the variance of the fused sensory measurement, $\sigma^2_{\hat{\theta}_t}$, and the variance of the motor command, $\sigma^2_u$. The input to the model (set by the experimental protocol) are the target goal direction, $G$, and the perceived direction of tactile motion, $T$, which we assumed to be always perpendicular to the orientation of the ridges. This introduces a bias in the perceived direction of motion whenever it is not perpendicular to the ridges. This phenomenon arises from the putative mechanism of motion encoding in touch, akin to the aperture problem in vision (*16*). The weight of tactile signals $w_T$ reflects the reliance that the observer has on touch compared to proprioception, which in Bayesian framework is a function of the variance of the two signals. We simulated the results of Exp. 2, where participants attempted to move straight ($G = 0$) with and without the rubber glove, and of Exp. 3, where participants reached for the different target goals ($G = [-15, 0, 15]$). Exp. 1 is identical to the without-glove condition tested in Exp. 2; therefore, it would redundant simulating both of them. To simulate the without-glove condition of Exp. 2 and 3, we set $w_T = 0.15$. This is in accordance with previous studies that showed a smaller weight of touch compared with proprioception for the estimate of hand displacement (*6*, *7*). We reduced the tactile weight to simulate the with-glove condition, $w_T = 0.05$, since it is known that wearing the glove reduces the reliability of the tactile signal (*21*). We set $\sigma^2_{\hat{\theta}_t}$ and $\sigma^2_u$ by trial and error to 50 and 1, respectively. The variance of the current state estimate was initialized to 10, and was updated at each iteration according to the equations of the Kalman filter (*26*).

Simulated data reproduced relevant features of the participants' motor behavior. As illustrated in Fig. 5A, the motion direction changed with the orientation of the ridges. For each simulated trial, we computed the motion angle and fit the relationship with the ridge orientation with a linear model, as explained for Exp. 1-3. As shown in Fig. 5B, the effect of ridge orientation was statistically significant (slope: $-0.17 \pm 0.005$, $p < 0.001$). The effect size decreased with the weight of the tactile signal, mimicking the difference between glove and no-glove conditions in Exp. 2 (slope difference: $0.11 \pm 0.007$, $p < 0.001$). Next, we simulated a task akin to Exp. 3, with three different targets to change the goal direction (Fig. 5C). In accordance with real data, the motion direction changed with the orientation of the ridges (slope: $-0.17 \pm 0.003$, $p < 0.001$) and with the position of the target (shift: $1.1 \pm 0.01$, $p < 0.001$).

[Fig. 5 about here]

## Discussion

This study demonstrates that touch provides an important feedback about limb position and displacement for motor control. We used a simple reaching task where we dissociated redundant cues from touch and proprioception while sliding a finger against a ridged surface, by manipulating the orientation of the ridges. This produced a robust and systematic deviation in reaching movements that support the hypothesis that touch complements proprioception in active motor control. Behavioural results are consistent with an ideal observer model that takes into account somatosensory input at different levels: From skin deformation (slip motion perpendicular to the ridges produces most of the tissue strain, as explained in the tactile flow model) to prior assumption (inanimate objects are assumed to be stationary) and motor control (efference copy, sensory integration) (*9*, *15*, *16*). The behavioral results in Exp. 2 show that the weight of proprioception and touch in the fused estimate depends on the reliability of each of the two signals, in accordance with the hypothesis of optimal cue integration in motor control.

According to a classical view in neuroscience, the main role of touch is to encode properties of the external world. Examples are the weight and the mass of objects, their texture, softness, shape, friction coefficient, and movement (*3*, *13*, *27–30*). In this view, exteroception (the perception of the status of the external world) and proprioception (the perception of motion status and posture of our own body) are two independent functions of the somatosensory system (*1*, *4*, *31*). The present results suggest a new intriguing view, where the two processes of exteroception and proprioception are connected at a functional level. If the observer is provided with "enough" evidence that the surface is stationary (for e.g. from prior knowledge or other senses), he or she will use tactile signals to get a redundant estimate of hand motion. We are all familiar with this in our daily life: When we move indoors with eyes closed or in the dark, the contact of our outstretched arms with the wall informs us on our position with respect to the boundaries of the navigation space. The present results demonstrate that the contribution of cutaneous information for motor control goes well beyond simply providing a stop signal: In conditions such as those exemplified by the experimental tasks, and when the properties of the world are known or assumed, touch dynamically guides reaching movement towards the desired targets. The interplay between touch and proprioception at a functional level complement neuroimaging studies showing the interaction between musculoskeletal and cutaneous signals in the primary somatosensory cortex (*32*).

This novel view of touch as a cue for proprioception seems at odds with the well-established phenomenon of tactile suppression, where observers' sensitivity to tactile stimuli is decreased during action (*33*). Results of the current study suggest that tactile suppression might not be a general phenomenon: Stimuli used to demonstrate tactile suppression classically include vibrations or electric stimulation of the skin, which are irrelevant for the control of movement and therefore are missed (i.e., suppressed) by the agent. Instead, the present results demonstrate that, rather than being suppressed, tactile cues naturally associated to the task systematically influence motor control.

Given that in this study we manipulated the orientation of the surface ridges, it may be argued that motor biases would arise from frictional and reaction forces pushing the hand away from the target. This alternative explanation can be ruled out based on two lines of evidence. First, participants only exerted weak forces on the plate (overall less than 1N) and we did not find any significant relationship between the contact force and the angular error. Even in the control experiment, where we minimized the frictional forces by lubricating the surface, we observed a significant deviation with respect to the target direction. Second, if the reaction force produced by the ridges caused deviations from target direction, participants would move about parallel to the ridges (or the grooves), and the angular error would be larger at +/- 30° than at +/- 60°, which is the opposite of what we found (Figure S6). Therefore, it seems reasonable to conclude that the systematic errors in hand trajectory depend on the mechanism of sensory coding and motor control (as also postulated by the observer model), rather than on purely mechanical factors related to frictional and reactions forces between the finger and the ridged surface.

Combining proprioceptive and tactile signals requires calibrating motion estimates between two frames of reference; namely, the linear motion with respect to the skin (for touch) and the angular motion in the joint and muscle space (for proprioception). Our somatosensory system, like other senses, has a poor spatial constancy, that is, it performs poorly when combining motion estimate of the movable sensor (the hand) with motion across the sensory sheet (the skin). This may explain why, in tasks requiring the discrimination of object motion, we provide more accurate judgements when keeping the hand stationary (*9*). In contrast, as discussed above, using touch as a contact proprioceptive cue leverages on the intrinsic assumption of the static nature of objects. For an ideal observer, this assumption holds if the hand velocity (for e.g., as encoded by receptors in the musculoskeletal system) is equal and opposite of tactile velocity. Recent studies–including the current results–suggest that the criterion above is not followed strictly, that is, the observer integrates proprioceptive and tactile cues despite small discrepancies between the two estimates. For instance, studies where the surface was moved by a tactile display suggest that the static nature of objects can be assumed a priori, rather than measured online (*9*). Still, it is possible that integration would break for larger discrepancies between the two motion estimates. In the current reaching experiments, we focused on translational motion of the fingertip, however it has been documented that illusory sensation of hand rotation can be also induced by a rotation of the contact surface on the palm in passive perceptual tasks (*6*). It will be interesting to test for the generalizability of the current results to the case of rotational movements.

Several neurological diseases—including diabetic neuropathy, traumatic nerve injuries, multiple sclerosis, and Guillain-Barré syndrome, to mention a few—cause dysfunctions in cutaneous touch, such as paresthesia (abnormal sensation such as tingling or tickling) and hypoesthesia (reduced tactile sensitivity) (*1*, *10*). There have been a number of reports of patients with purely sensory deficits. For instance, patients I.W. and G.L. lost sensation of touch and muscular proprioception as the consequence of a peripheral neuropathy selective for the large myelinated fibers (*10*). Despite the motor nerves being intact, these patients present severe motor impairment due to the lack of somatosensory feedback. Unraveling the contribution of touch for the control of movement may provide a better understanding of the physiopathology of these diseases, and pave the path for the development of more sensitive clinical tests. For example, as observed in Exp. 2, the dependency of the motion trajectory on the orientation of the ridges scales with tactile sensitivity. For this reason, the reaching tasks used for this study may have a potential application for the quantitative assessment of tactile deficits. The severity of tactile dysfunction would correlate with the capacity of moving straight in our task, and this could be quantified by the slope of the linear relationship in Fig. 2C.

Marr argued that to fully describe a system it is important to understand the goals of its computations (*34*). While a classic view in neuroscience calls for a functional separation between exteroception and proprioception, this study supports the alternative hypothesis that these two goals are instead functionally connected. By shedding light on the overarching goals of somatosensory processing, the current results provide a better understanding of the computations performed by human somatosensory system.

## Materials and Methods

### Participants

Thirty-nine naïve participants completed our behavioral experiments: Ten participants took part in Exp. 1 (4 males and 6 females, $25 \pm 1.3$ years of age, mean $\pm$ standard deviation), twenty-one participants in Exp. 2 (10 males and 11 females, $27 \pm 1.5$ years of age), and eight in Exp. 3 (5 males and 3 female, $28 \pm 3$, years of age). The sample size was set in accordance with previous studies in haptic literature (e.g., (*2*, *9*)). We performed a power analysis with the parameters set in accordance with our preliminary results (*35*, *36*); in the three experiments, the power was above 80% (see Supplemental Data). All participants were right-handed and reported no medical condition that could have affected the experimental outcomes. Informed written consent was obtained from all participants involved in the study. The testing procedures were approved by the Ethical Committee of the University of Pisa, in accordance with the guidelines of the Declaration of Helsinki for research involving human subjects.

### Stimulus and Procedure

The experimental setup is illustrated in Fig. 1A. The contact surface consisted of a 3D-printed circular plate, having a diameter of 15 cm. The plate had a textured surface with regularly spaced ridges. The size and the spacing of the ridges was the same as in (*16*) (ridge height and width: 1 mm; space between ridges: 10 mm). The plate was placed over a load cell (Micro Load Cell, 0 to 780 g, CZL616C from Phidgets, Calgary, AB-Canada) to record normal contact forces. A servo motor (Ultra Torque HS-7950TH by HITEC) under the plate rotated it at the required orientation. For hand tracking, a Leap Motion device (Leap Motion Inc., San Francisco, U.S.) was attached to a handle placed above the plate. The current study focused on translational motion; therefore, we only tracked a single point on the tip of the finger. The sampling frequency of the Leap Motion device is equal to 40 Hz, and its accuracy in dynamic conditions is equal to 1.2 mm, allowing reliable tracking of hand and finger motion (*37*).

The procedure in Exp. 1 was the following. Blindfolded participants sat on an office chair in front of the setup, with the centre of the plate roughly aligned with their body mid-line. Headphones playing pink noise masked occasional ambient sounds. Before each trial, the experimenter placed the right index fingertip of the participant in contact with the plate, on the ridge closest to the nearer edge of the plate. Thereafter, participants were required to slide the hand away from them along a straight path, for approximately 10 cm (Fig. 1B). Participants were instructed to contact the plate with a light touch. Prior to each trial, the plate was rotated by the motor to one of the following angular position: $-60°$, $-30°$, $0°$, $30°$, $60°$. As illustrated in Fig. 1D, a zero angle means that the ridges of the plate were parallel to the frontal plane of the participant, whereas negative (positive) angles means that the ridges were rotated clockwise (counterclockwise). Each stimulus orientation was presented fifteen times in pseudo-random order. Participants received no feedback about their performance during the experiment. At the end of each trial, the experimenter lifted the hand of the participant to place it back to the starting position. Before the experimental session, participants underwent a training phase, where the experimenter instructed them to produce the right amount of force and hand displacement. During training, participants received feedback whenever the actual force exceeded the threshold value of 2 N. All participants replicated the task with a smooth plate without ridges. The order of the ridged- and the smooth-plate conditions was counterbalanced across participants. This aimed at correcting our results for possible biases in perceived direction introduced by extra-cutaneous signals, see for e.g. (*38*, *39*). Additionally, to address the role of frictional force, a subset of participants (n = 4) replicated the task with a lubricated surface (Exp. 1b). This time, before each experimental session, the plate was lubricated using oil (ridged-plate condition only).

In Exp. 2, participants performed the same task of Exp. 1 either with their bare finger, or while wearing a rubber glove reducing the reliability of the tactile stimulus. The two conditions, with and without glove, were tested in two experimental sessions, counterbalanced across participants. In each session, each of the five orientations of the plate was presented ten times, in pseudo-random order. Before each experimental session, we verified that participants were able to feel the ridges while wearing the glove.

In Exp. 3, the ridged plate was aligned with the right shoulder of the participant to reduce the offset due to extra-cutaneous signals. Participants wore a Head Mounted Display (HMD; Oculus Rift by Oculus VR, LLC) to present the visual stimuli. The virtual scene consisted of a circular plate having the same size and position as the real plate, without ridges (Fig. 3A). Prior to the experiment, the virtual plate has been aligned in space with the real one by combining signals of the Leap Motion and the virtual scene rendered through the Oculus Rift. At the trial onset, the experimenter placed the finger of the participant on the real plate on the starting point. Thereafter, a visual target consisting of a green sphere (radius = 1 cm) briefly flashed on the virtual plate. The visual target was placed on the arc of an ideal circumference with radius of 5 cm, in one of the following angular position: $-15°$, $0°$, $15°$ (Fig. 3A). Participants were instructed to slide the hand over the textured plate to reach the target. Prior to each trial, the plate was rotated by the motor to one of the following angular position: $-60°$, $0°$, $60°$ with respect to the virtual target. A zero angle means that the ridges of the plate were orthogonal to the line joining the starting point and the target, whereas negative (positive) angles means that the ridges were rotated clockwise (counterclockwise). Ridges were not displayed on the virtual disk, which had a uniform color. Participants did not receive any feedback whether they reached or not the target. A "beep" sound alerted the participants when they reached a distance from the origin equal to 10 cm. Whenever the contact force exceeded the threshold value of 2 N, a different sound alerted the participant to decrease the applied force. Before the experiment, a short training session allowed participants to familiarize with the apparatus and to reproduce the required motion speed and contact force. During the training session, the smooth plate was used.

In none of the experiments did we provide feedback on the motion speed. Participants were simply required to move along the goal direction with a slow self-paced hand movement. Before the experiment, however, the experimenter performed the movement once to show the participants the approximate range of speed and displacement.

## Data Analysis

The hand trajectory was recorded with the tracking system of the apparatus and saved for the analysis. The angular deviation from a straight-ahead motion direction (i.e., the deviation from the solid arrow in Fig. 1B, referred to as the motion angle) was computed from the position data as $\arctan(y/x)$, where $x, y$ are the coordinates of the final hand position. Negative (positive) angles indicates that the motion path rotated clockwise (counterclockwise) with respect to the solid arrow in the figure. In Exp. 1, we applied a Linear Mixed Model (LMM) to evaluate whether the orientation of the ridges, **X**, predicted the motion angle, **A** (*40*). Model equation was the following:

**(1)** $\mathbf{A} = \beta_0 + u_0 + (\beta_1 + u_1)\mathbf{X} + \epsilon,$

where $\beta_0$ and $\beta_1$ are the fixed-effect intercept and slope, respectively, $u_0$ and $u_1$ are the random-effect intercept and slope of the model (between-participant variability), and $\epsilon$ is the residual error term. We accounted for possible biases produced by extra-cutaneous signals, as follows. First, we tested whether the motion angle was significantly different between trials with a zero-degree orientation of the ridged plate (i.e., orthogonal to the required hand motion) and with the smooth plate. As the difference was not statistically significant (Likelihood Ratio Test, $p > 0.05$), these two conditions were pooled together for the analysis. Next, we fitted the following model to estimate the angular deviation from straight direction in the absence of biasing tactile stimuli.

**(2)** $\mathbf{A_0} = \beta_0^* + u_0 + \epsilon,$

where $\mathbf{A_0}$ is the predicted angle with zero-oriented or no ridges, and $\beta_0^*$ is the estimate of the possible bias due to extra-cutaneous signals. We used $\beta_0^*$ to correct the estimate of the tactile bias estimated in model. Linear Mixed Models were also used in Exp. 2 to evaluate the effect of the orientation of the ridges (**X**) on the angular deviation from straight direction (**A)**, and how the presence of the glove (**G**) modulated the phenomenon. In particular, we tested the interaction between ridges and glove (**XG**) to evaluate whether the slope of the linear regression changed between the two conditions:

**(3)** $\mathbf{A} = \eta_0 + u_0 + (\eta_1 + u_1)\mathbf{X} + (\eta_2 + u_2)\mathbf{XG} + \epsilon,$

where $\eta_0$ - $\eta_2$ are the fixed-effect parameters, $u_0$ - $u_2$ are the random-effect parameters (between-participant variability), and $\epsilon$ is the residual error term. In Exp. 3, we evaluated whether the orientation of the ridges, **X**, and the position of the visual target, **V**, predicted the angular deviation from the mid-line, **A**:

**(4)** $\mathbf{A} = \theta_0 + u_0 + (\theta_1 + u_1)\mathbf{X} + (\theta_2 + u_2)\mathbf{V} + \epsilon,$

In all LMMs, we tested the significance of the fixed-effect parameters by means of the Likelihood Ratio Test. Data analysis was performed in R language (R version 3.4.4). The R Package *lme4* was used to fit LMM.

## Optimal Observer Model

The optimal observer model evaluates the effect of the orientation of the ridges, of the goal direction, and of the reliability of tactile signal on the direction of hand motion. We used the same notation as (*26*), tailored to the issue of the current study. Refer to Table 1 for the list of symbols used in the model equations. The term $G$ indicates the goal direction, which is either straight ahead in Exp. 1–2 (goal direction, $G = 0°$) or towards a virtual target in Exp. 3 ($G = [-15°, 0°, 15°]$). At time *t*, the internal state of the system, $\hat{X}_t$ , is the estimate of the motion direction of the hand (one-dimensional variable). The ideal observer adjusts his or her direction of motion to compensate for the difference between the state estimate, $\hat{X}_t$, and the goal direction, $G$. To link the (measured) motor behaviour and the (latent) observer model, we assumed that the change in the direction of motion in the unitary time interval, $\Delta\theta$, is equal to the motor command, $u_t$. As illustrated in Fig. 4, a forward model predicts the next motion direction as the sum of the state estimate and the motor command:

$$\hat{X}^-_{(t+1)} = \hat{X}_t + u_t$$

The output of the forward model is compared with the direction of hand motion as measured by the somatosensory system, $\widehat{\theta}_{(t+1)}$, obtaining the following error term:

$$E = \widehat{\theta}_{(t+1)} - \widehat{X}^{-}_{(t+1)}$$

The measured direction is equal to a weighted sum of the two sensory signals from proprioception and touch, $P$ and $T$, respectively:

$$\widehat{\theta}_{(t+1)} = w_T T_{(t+1)} + w_P P_{(t+1)}$$

We assumed that the two weight terms, $w_T$ and $w_P$, are constant within each experimental session. To a first approximation, we assumed that the proprioceptive signal provides an accurate estimate of the actual direction of hand motion, that is, $\overline{P} = \theta$. Instead, the estimate from touch, $T$, is always orthogonal to the orientation of the ridges, in accordance with previous literature (*16*, *17*). Finally, the state estimate is updated based on the error term:

$$\widehat{X}_{(t+1)} = \widehat{X}^{-}_{(t+1)} + \mathrm{K}_{(t+1)}(E)$$

where $\mathrm{K}_{(t+1)}$ is the Kalman gain ($0 \leq \mathrm{K}_{(t+1)} \leq 1$). At time *t+1*, the Kalman gain is computed as:

$$\mathrm{K}_{(t+1)} = \frac{\sigma^2_{\widehat{X}^{-}_{(t+1)}}}{\sigma^2_{\widehat{X}^{-}_{(t+1)}} + \sigma^2_{\widehat{\theta}_{(t+1)}}}$$

where $\sigma^2_{\widehat{X}^{-}_{(t+1)}}$ is the variance of the forward model and $\sigma^2_{\widehat{\theta}_{(t+1)}}$ the variance of the sensory measurement. According to the model, a perceived deviation from the goal direction for e.g. to the left, $\widehat{\theta}_t > 0$, produces an update in the state estimate, triggering a correction movement to the right, and vice-versa. Participants do not apply corrections to the motion direction if either $E$ or $\mathrm{K}$ are equal to zero.

We simulated the outcome of the model and evaluated whether the response of the ideal observer matched the real data. In each simulated experiment, we simulated 75 trials including five plate orientations with 15 repetitions each. Each trial consisted of a simulated hand trajectory divided in 100 discrete steps of unitary length. The three free parameters of the model and the model input (motor goal and ridge orientation) were set as explained in the Result section. In each step, we updated the direction of motion, $\theta_t$ (which is the output of the simulation), by adding the change in direction occurred during the unitary interval, $\Delta\theta_{(t+1)}$:

$$\theta_{(t+1)} = \theta_t + \Delta\theta + \epsilon_{(t+1)}$$

with $\Delta\theta = u_t$. In the equation above, $\epsilon_{(t+1)}$ is the sum of the error term related to motor noise, $\epsilon_{(u_t)}$, and one related to the noise of the state estimate, $\epsilon_{(\widehat{X}_t)}$. The two error terms were sampled from two Gaussian distributions with parameters $N(0, \sigma^2_{u_t})$ and $N(0, \sigma^2_{\widehat{X}_t})$, respectively. The variance of the internal estimate, $\sigma^2_{\widehat{X}_t}$, the variance of the forward model, $\sigma^2_{\widehat{X}^{-}_{(t+1)}}$, and the Kalman gain, $K_{(t+1)}$, were computed in each iteration following Kalman filter equations (*26*).

Simulated data were generated in R language (R version 3.4.4).

## References

1. E. P. Gardner, K. O. Johnson, in *Principles of Neural Science*, E. R. Kandel, J. H. Schwartz, T. M. Jessel, S. A. Siegelbaum, A. J. Hudspeth, Eds. (McGraw-Hill, New York, Fifth., 2013), pp. 451–471.
2. J. A. Pruszynski, R. S. Johansson, J. R. Flanagan, A Rapid Tactile-Motor Reflex Automatically Guides Reaching toward Handheld Objects. *Curr. Biol.* **26**, 788–792 (2016).
3. S. J. Lederman, R. L. Klatzky, Extracting object properties through haptic exploration. *Acta Psychol. (Amst).* **84**, 29–40 (1993).
4. U. Proske, S. C. Gandevia, The Proprioceptive Senses: Their Roles in Signaling Body Shape, Body Position and Movement, and Muscle Force. *Physiol. Rev.* **92**, 1651–1697 (2012).
5. B. B. Edin, J. H. Abbs, Finger movement responses of cutaneous mechanoreceptors in the dorsal skin of the human hand. *J. Neurophysiol.* **65**, 657–70 (1991).
6. C. Blanchard, R. Roll, J.-P. Roll, A. Kavounoudias, Combined contribution of tactile and proprioceptive feedback to hand movement perception. *Brain Res.* **1382**, 219–229 (2011).
7. A. Moscatelli *et al.*, The Change in Fingertip Contact Area as a Novel Proprioceptive Cue. *Curr. Biol.* (2016), doi:10.1016/j.cub.2016.02.052.
8. A. V Terekhov, V. Hayward, The brain uses extrasomatic information to estimate limb displacement. *Proc. R. Soc. B Biol. Sci.* **282**, 20151661 (2015).
9. A. Moscatelli, V. Hayward, M. Wexler, M. O. Ernst, Illusory Tactile Motion Perception: An Analog of the Visual Filehne Illusion. *Sci. Rep.* **5**, 14584 (2015).
10. J. Cole, J. Paillar, in *The Body and the Self* (The MIT Press, Cambridge, 1998), pp. 245–266.
11. M. A. Goodale, A. D. Milner, Separate visual pathways for perception and action. *Trends Neurosci.* (1992), , doi:10.1016/0166-2236(92)90344-8.
12. M. P. M. Kammers, I. J. M. van der Ham, H. C. Dijkerman, Dissociating body representations in healthy individuals: Differential effects of a kinaesthetic illusion on perception and action. *Neuropsychologia*. **44**, 2430–2436 (2006).
13. J. Platkiewicz, V. Hayward, Perception-Action Dissociation Generalizes to the Size-Inertia Illusion. *J. Neurophysiol.* **111**, 1409–16 (2014).
14. D. Wolpert, Z. Ghahramani, M. Jordan, An internal model for sensorimotor integration. *Science (80-. ).* **269**, 1880–1882 (1995).
15. D. M. Wolpert, K. G. Pearson, C. P. J. Ghez, in *Principles of Neuroscience*, E. R. Kandel, J. H. Schwartz, T. M. Jessel, S. A. Siegelbaum, A. J. Hudspeth, Eds. (McGraw-Hill, New York, Fifth., 2013), pp. 743–767.
16. A. Bicchi, E. P. Scilingo, E. Ricciardi, P. Pietrini, Tactile flow explains haptic counterparts of common visual illusions. *Brain Res. Bull.* **75**, 737–741 (2008).
17. Y. C. Pei, S. S. Hsiao, S. J. Bensmaia, The tactile integration of local motion cues is analogous to its visual counterpart. *Proc. Natl. Acad. Sci. U. S. A.* **105**, 8130–8135 (2008).
18. J. Burge, M. O. Ernst, M. S. Banks, The statistical determinants of adaptation rate in human reaching. *J. Vis.* **8**, 20 (2008).
19. K. P. Kording, D. M. Wolpert, Bayesian integration in sensorimotor learning. *Nature*. **427**, 244–247 (2004).
20. M. O. Ernst, M. S. Banks, Humans integrate visual and haptic information in a statistically optimal fashion. *Nature*. **415**, 429–33 (2002).
21. R. R. Bishu, G. Klute, in *Proceedings of the 36th Annual Human Factors and Ergonomic Society Conference* (Seattle, 1993; https://ntrs.nasa.gov/search.jsp?R=19940011244).
22. A. Moscatelli, M. Mezzetti, F. Lacquaniti, Modeling psychophysical data at the population-level: The generalized linear mixed model. *J. Vis.* **12**, 26–26 (2012).
23. H. Kinoshita, Effect of gloves on prehensile forces during lifting and holding tasks.

*Ergonomics*. **42**, 1372–1385 (1999).
24. P. Morasso, Spatial control of arm movements. *Exp. Brain Res.* **42**, 1–5 (1981).
25. J.-J. Orban de Xivry, S. Coppe, G. Blohm, P. Lefevre, Kalman Filtering Naturally Accounts for Visually Guided and Predictive Smooth Pursuit Dynamics. *J. Neurosci.* **33**, 17301–17313 (2013).
26. P. S. Maybeck, Stochastic models, estimation, and control. *New York*. **1**, 1–16 (1979).
27. W. M. Bergmann Tiest, A. M. L. Kappers, Haptic perception of gravitational and inertial mass. *Attention, Perception, Psychophys.* **72**, 1144–1154 (2010).
28. D. Gueorguiev, E. Vezzoli, A. Mouraux, B. Lemaire-Semail, J.-L. Thonnard, The tactile perception of transient changes in friction. *J. R. Soc. Interface*. **14**, 20170641 (2017).
29. M. Salada, P. Vishton, J. E. E. Colgate, E. Frankel, in *12th International Symposium on Haptic Interfaces for Virtual Environment and Teleoperator Systems, 2004. HAPTICS '04. Proceedings.* (IEEE, 2004; http://ieeexplore.ieee.org/xpls/abs_all.jsp?arnumber=1287190), pp. 146–153.
30. F. Fardo, B. Beck, T. Cheng, P. Haggard, A mechanism for spatial perception on human skin. *Cognition*. **178**, 236–243 (2018).
31. H. P. Saal, S. J. Bensmaia, Touch is a team effort : interplay of submodalities in cutaneous sensibility. *Trends Neurosci.* **37**, 689–697 (2014).
32. S. S. Kim, M. Gomez-Ramirez, P. H. Thakur, S. S. Hsiao, Multimodal Interactions between Proprioceptive and Cutaneous Signals in Primary Somatosensory Cortex. *Neuron*. **86**, 555–566 (2015).
33. C. E. C. E. Chapman, M. C. M. C. Bushnell, D. Miron, G. H. Duncan, J. P. Lund, Sensory perception during movement in man. *Exp. Brain …*. **68**, 516–524 (1987).
34. D. Marr, *Vision: A computational investigation into the human representation and processing of visual information* (W. H. Freeman and Company, New York, NY, 1982).
35. M. Bianchi *et al.*, in *2017 IEEE World Haptics Conference (WHC)* (IEEE, 2017; http://ieeexplore.ieee.org/document/7989883/), pp. 96–100.
36. G. C. Bettelani, A. Moscatelli, M. Bianchi, in *2018 7th IEEE International Conference on Biomedical Robotics and Biomechatronics (Biorob)* (Twente, 2018), pp. 2–6.
37. F. Weichert, D. Bachmann, B. Rudak, D. Fisseler, Analysis of the Accuracy and Robustness of the Leap Motion Controller. *Sensors*. **13**, 6380–6393 (2013).
38. A. M. L. Kappers, J. J. Koenderink, Haptic Perception of Spatial Relations. *Perception*. **28**, 781–795 (1999).
39. C. T. Fuentes, A. J. Bastian, Where Is Your Arm? Variations in Proprioception Across Space and Tasks. *J. Neurophysiol.* **103**, 164–171 (2010).
40. D. Bates, M. Mächler, B. Bolker, S. Walker, Fitting Linear Mixed-Effects Models Using lme4. *J. Stat. Softw.* **67**, 1–51 (2015).

## Acknowledgments

**General**: We thank Priscilla Balestrucci, Irene Senna, Barbara La Scaleia, Marc O. Ernst, and Massimiliano Di Luca for helpful comments and suggestions. We thank Davide Doria for help with the experimental setup. Preliminary results of Exp. 1 (n = 6) and Exp. 2 (n = 7) have been presented, respectively, at IEEE World Haptic Conference, 2017 (*35*), and at BioRob Conference, 2018 (*36*).

**Funding:** This work is partially supported by Facebook Reality Lab (Facebook Inc.), and by the European Union - Horizon 2020 research and innovation program, under grant agreement No. 688857 (SoftPro).

**Data Availability.** The datasets generated during and/or analysed during the current study are available from the corresponding authors on reasonable request.

**Author contributions:** A.M., M.B. and S.C. conceived and designed the experiments. M.B., S.C., and G.C.B. implemented the setup and performed the experiments. A.M. analyzed the data. A.M., M.B., G.C.B., S.C. and C.V.P. developed the explanatory model. All authors interpreted results of experiments. A.M., C.V.P. and M.B. drafted the manuscript. All authors edited, revised, and approved the final version of the manuscript.

**Competing interests:** The authors have declared that no competing interests exist.

## Figures and Tables

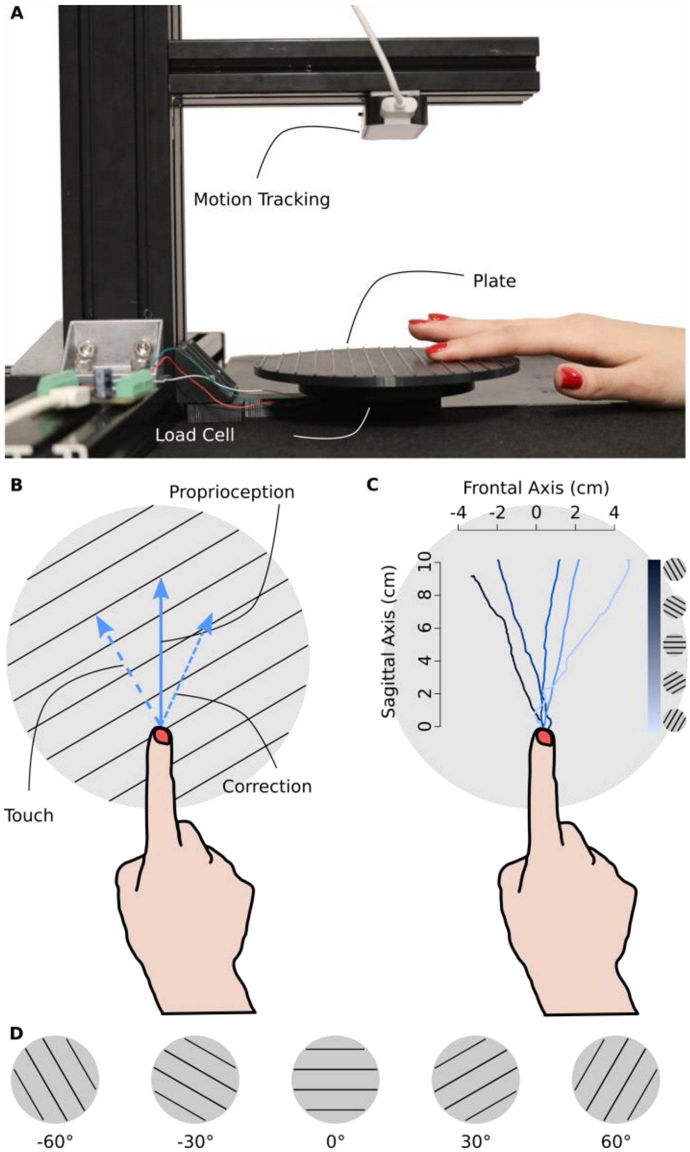


**Fig. 1. Experimental Setup and Protocol.** (**A**) The experimental setup including the textured circular plate, the load cell, and the motion tracking system. In each trial, the servomotor placed under the plate (not visible in the picture) set the orientation of the plate. (**B**) Blindfolded participants were asked to slide their finger over the ridged plate, along a straight direction away from their body mid-line. We assumed that extra-cutaneous proprioceptive cues provided an accurate measurement of motion direction (solid arrow). Instead, the cutaneous feedback produced an illusory sensation of bending towards a direction perpendicular to the ridges, in accordance with previous literature (dashed arrow). This eventually led to an adjustment of the motion trajectory towards the direction indicated by the dotted arrow. (**C**) Example of trajectories with different ridges. Data from a single participant. (**D**) Plate orientations ranged from $-60^{\circ}$ to $60^{\circ}$.

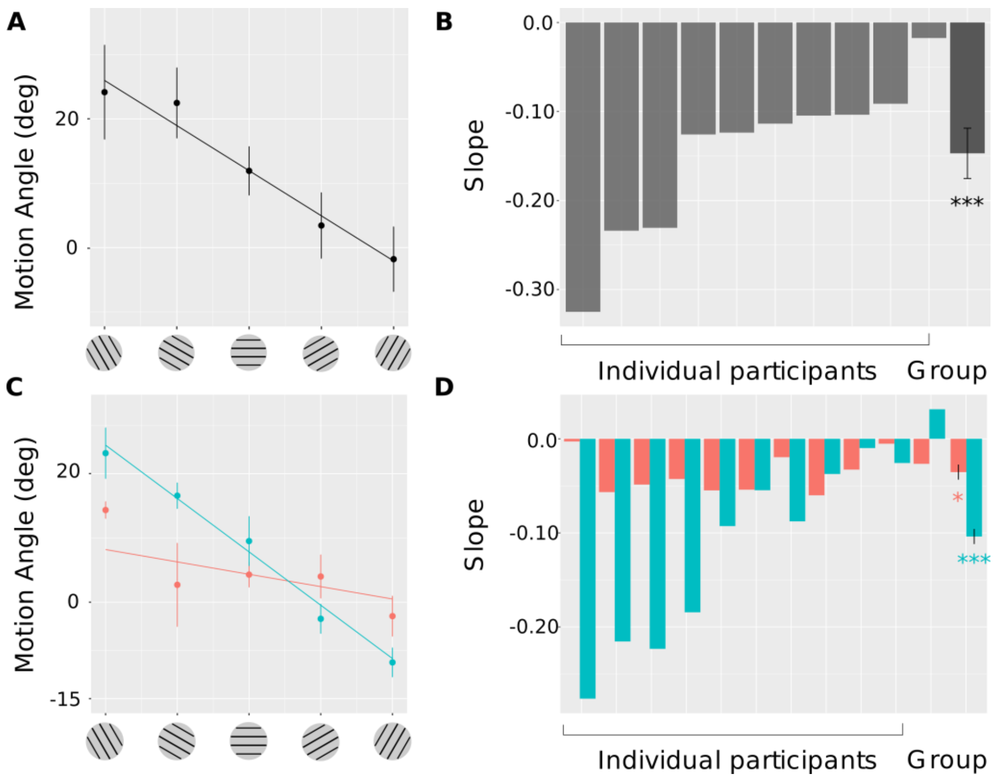


**Fig. 2. Results of the Exp. 1-2.** (**A**) Exp. 1, the motion angle of the hand trajectory with respect to body mid-line regressed against the orientation of the textured plate. Positive y values are for a leftward deviation from the mid-line, whereas negative values for a rightward deviation. In accordance with our predictions, there is a negative relationship (negative slope) between the error and the plate orientation. Data and liner fit from a representative participant. (**B**) The slope of the linear relationship for 10 participants with group estimate and standard deviation (LMM estimates). (**C-D**) Exp. 2, conditions with and without glove are represented as orange and azure lines/bars, respectively.

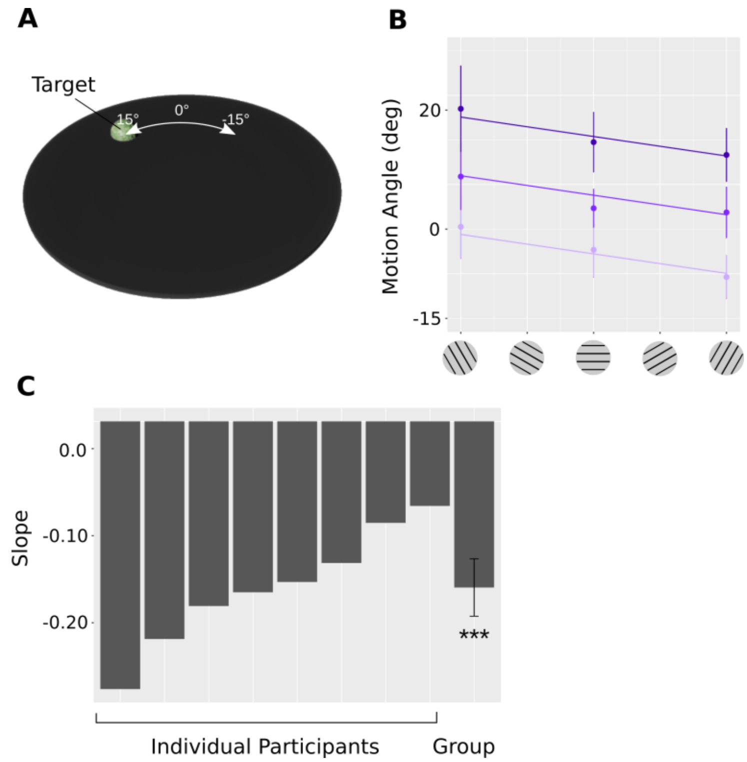


**Fig. 3. Stimuli and Results in Exp. 3**. **(A)** The virtual disk had the same size and position as the real plate. The visual target was arranged on the arc of an ideal circumference with radius of 5 cm on the plate, in one of the following angular position: −15°, 0°, 15°. The white arrow and the labels were not visible during the experiment. Visual stimuli were displayed by means of an HMD. **(B)** The position error of the hand trajectory with respect to body mid-line. The color code is for the different target position, with light, medium, and dark purple corresponding to −15°, 0°, and 15°, respectively. Plate orientation is w.r.t. the position of the target. Data from a representative participant. **(C)** The slope of the linear relationship for eight participants with group estimate and standard deviation (LMM estimates).

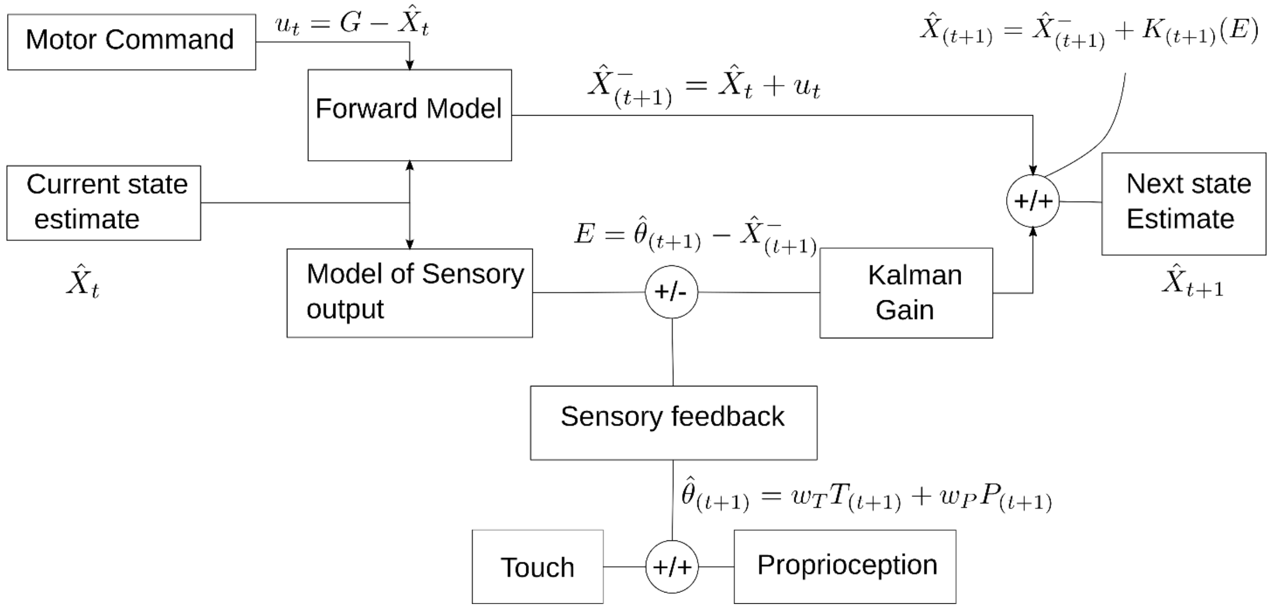


**Fig. 4: The Kalman filter model.** Based on the estimate of the current state and the motor command, a forward model predicts the following state of the limb. This internal estimate is compared to the sensory measurement, generating an error term. In our task, the sensory measurement is equal to the Bayesian integration of the proprioceptive and the tactile cues. This error term, weighted by a gain factor (the Kalman gain), is used to update the estimate of the system, and eventually corrects the motor command.

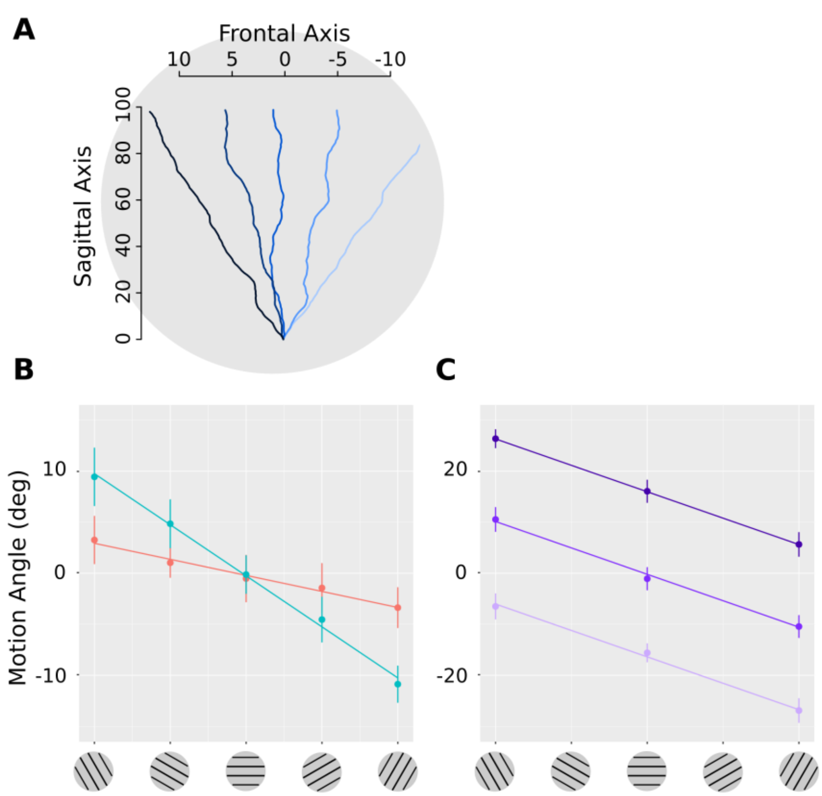


**Fig. 5: Simulated data from the Kalman filter model. (A)** The simulated trajectory **(B)** Simulation of Exp. 2. The tactile weight, $w_T$ was set to 0.15 and 0.05 to simulate the with- and the without-glove condition, respectively (with $w_P = 1 - w_T$). We used the same color code as for Exp. 2; with- and without-glove condition were represented in orange and azure, respectively. **(C)** Simulation of Exp. 3. The color code is for the different target

position, with light, medium, and dark purple corresponding to −15°, 0°, and 15°, respectively.

| | |
|---|---|
| $\theta$ | Actual motion angle |
| $\hat{\theta}$ | Measured motion angle |
| u | Motor command |
| $\hat{X}$ | State estimate |
| $\hat{X}^-$ | Forward model of the motor command |
| K | Kalman gain |

**Table 1. Parameters of the observer model.** For the sake of readability, the subscript indicating the discrete time interval (e.g., $\hat{X}_t$) was omitted in the table.

# Supplementary Information

**Title**

- Full title: "Touch as an auxiliary proprioceptive cue for movement control"
- Short titles "Touch as an auxiliary proprioceptive cue"


**Authors**

A. Moscatelli,[1,2]*[†] M. Bianchi[3]*[†], S. Ciotti, [3,5] G. C. Bettelani,[3] C.V. Parise[4], F. Lacquaniti[1,2], A. Bicchi[3,5].

**Affiliations**

[1]Department of Systems Medicine and Centre of Space Bio-medicine, University of Rome "Tor Vergata", Rome, Italy.
[2]Laboratory of Neuromotor Physiology, Fondazione Santa Lucia IRCCS, Rome, Italy.
[3]Centro di Ricerca "E. Piaggio" and Dipartimento Ingegneria dell'Informazione, University of Pisa, Pisa, Italy.
[4]Oculus Research, Redmond, Washington, United States of America.
[5]SoftBots Lab - Soft Robotics for Human Cooperation and Rehabilitation, Istituto Italiano di Tecnologia, IIT, Genoa, Italy

*a.moscatelli@hsantalucia.it; matteo.bianchi@centropiaggio.unipi.it

[†] These authors contributed equally to this work.


# Hand Displacement: LMM fit and Raw Data

Figure S1 illustrates the convention for the angles of the hand trajectory in Exp 1–3. Negative (positive) angles indicate that the motion path rotated clockwise (counterclockwise) with respect to the sagittal axis of the participant. Figures from S2 to S5 show the raw data and the model fit in Exp. 1–3. The angular deviation from a straight-ahead motion direction was computed from the position data as $\arctan(y/x)$, where $x, y$ are the coordinates of the final hand position. Linear Mixed Models (LMMs) have been used to fit the angular deviation of the hand trajectory as a function of the orientation of the grating, as explained in the manuscript. It is worth noting that participants were not following the ridges. If this were the case, the absolute error would have been larger for $\pm$ 30 deg stimuli and smaller for $\pm$ 60 deg, which was the opposite of what we found. This is further explained in figure S6.

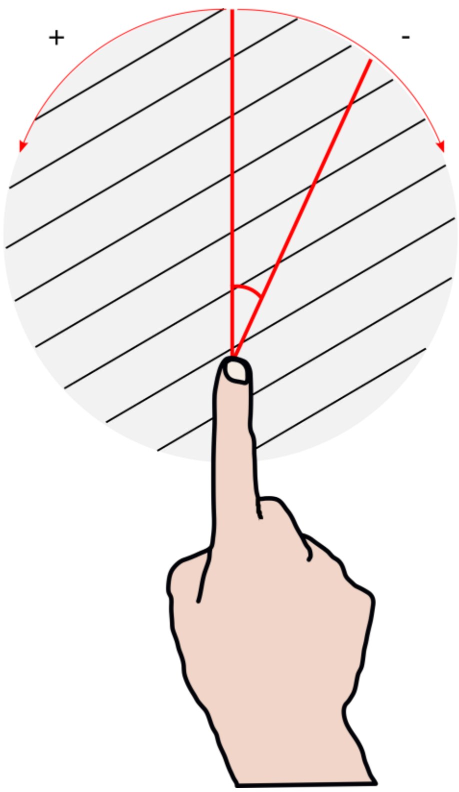


*Fig. S1. Convention for the angles of the hand trajectory in Experiment 1–3. Negative motion angles indicate that the hand trajectory was rotated clockwise with respect the body mid-line (sagittal axis), and vice versa. In other terms, a clockwise rotation means that the hand trajectory deviated rightwards, whereas a counterclockwise rotation means that it deviated leftwards.*

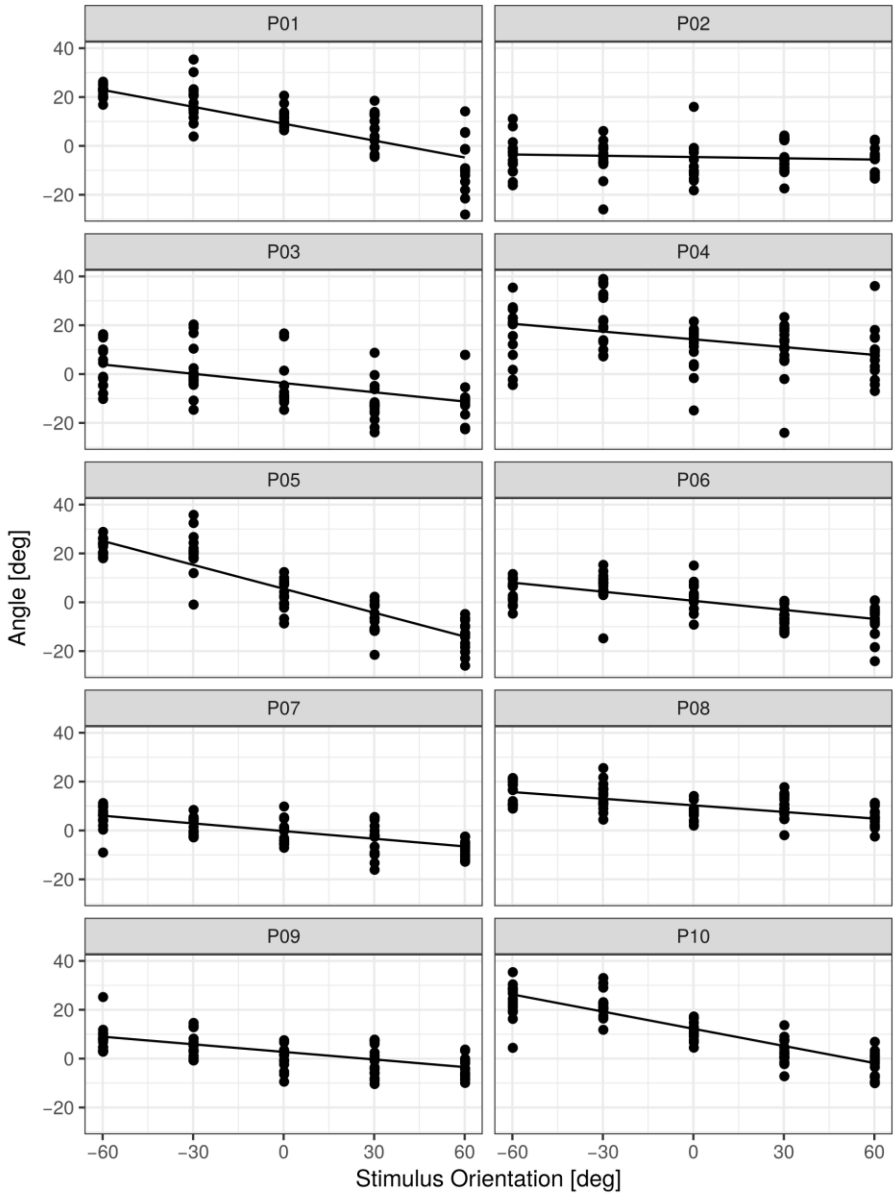


*Fig. S2. Exp. 1, the angular deviation of the hand trajectory as a function of the orientation of the grating in participants P01-P10. Point data for individual trial and LMM prediction.*

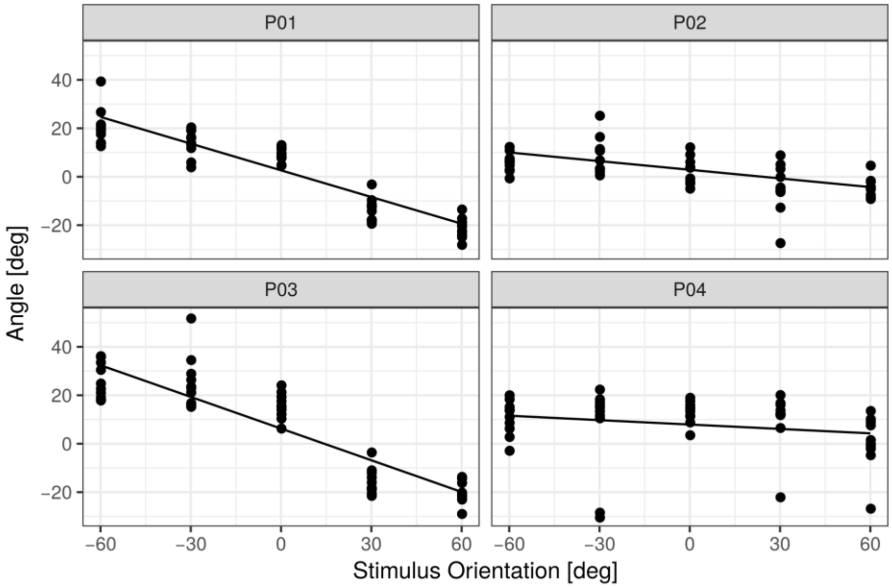


758

759 *Fig. S3. Exp. 1b (lubricated surface), the angular deviation of the hand trajectory as a function*
760 *of the orientation of the grating in participants P01-P04. Point data for individual trial and*
761 *LMM prediction.*

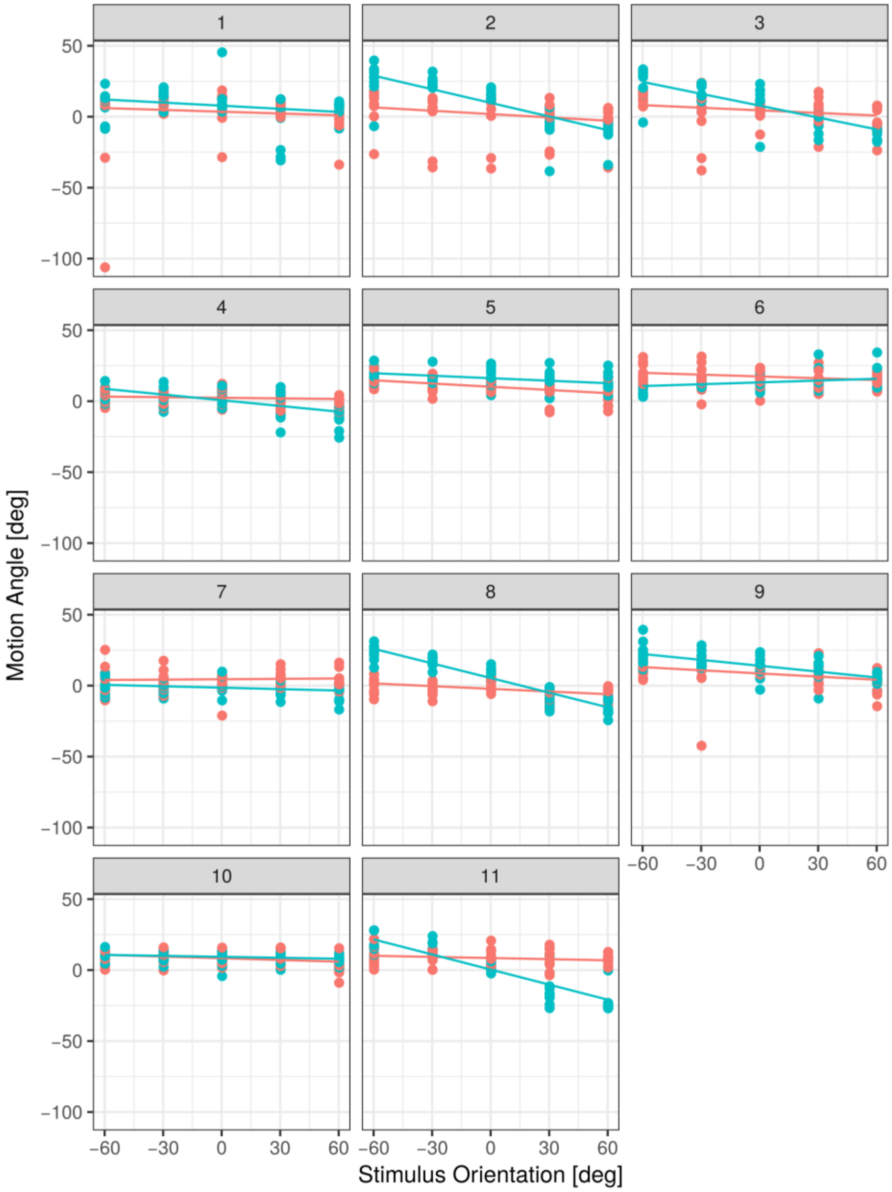


*Fig. S4. Exp. 2, the angular deviation of the hand trajectory as a function of the orientation of the grating in participants P01-P11. With and without glove conditions are represented in orange and azure, respectively. Point data for individual trial and LMM prediction.*

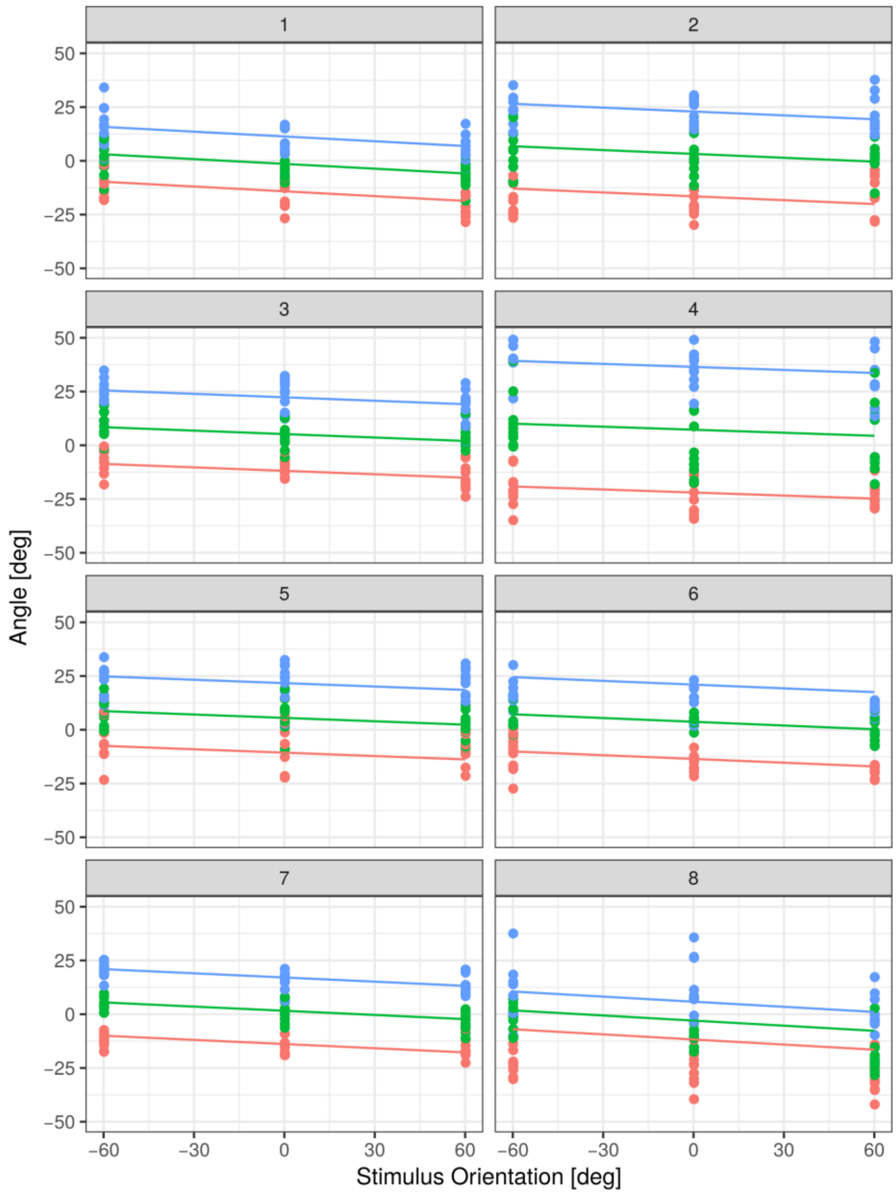


*Fig. S5. Exp. 3, the angular deviation of the hand trajectory as a function of the orientation of the grating in participants P01-P08. Different colors represent the visual target displayed in VR. Point data (individual trial) and LMM prediction.*

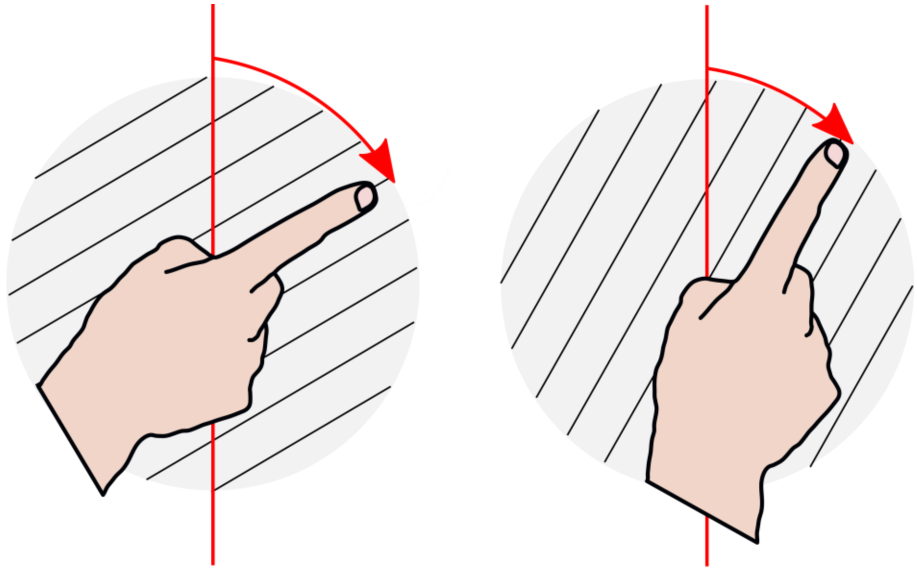


*Fig. S6. If participants were following the ridges, the absolute error would have been larger for ± 30 deg stimuli and smaller for ± 60 deg, which was the opposite of what we found.*

## Power Analysis

We used the R package SIMR that is specifically designed for power analysis of LMM models. To run the analysis, we assumed the effect size of the orientation of raised ridge (referred to a “slope” in the manuscript) equal to -0.15. This value was set in accordance with two pilot studies, presented at IEEE World Haptic Conference, 2017, and at BioRob Conference, 2018. First, we set the sample size to 10 participants for a total number of 750 trials; the analysis returned a statistical power above 90%. Next, we reduced the sample size to 450 trials with ridge orientation equal to -60 deg, 0, and 60 deg (as for a single target goal in Exp. 3); the power was still above 80%.

## Motion Velocity and Normal Force

We analyzed the motion velocity and normal force in the three experiments. Participants were required to move along the goal direction with a slow self-paced hand movement, and to stop before reaching the farther edge of the plate. Before the experiment, the experimenter performed the movement once to show the participants the approximate range of speed and displacement. Participants were required keeping the normal force below two N. Finger position and speed were recorded with the Leap Motion device (Leap Motion Inc., San Francisco, U.S.) attached to a handle placed above the plate. Normal force was recorded with a load cell (Micro Load Cell, 0 to 780 g, CZL616C from Phidgets, Calgary, AB-Canada) placed below the plate. The load cell was calibrated before each experimental session.

Raw velocity and force data were filtered each using a second order, Butterworth low-pass filter (cutoff frequency equal to 10 Hz). Figure S7 illustrates an example of Velocity (A) and Force (B) data from a representative trial (Exp. 1).

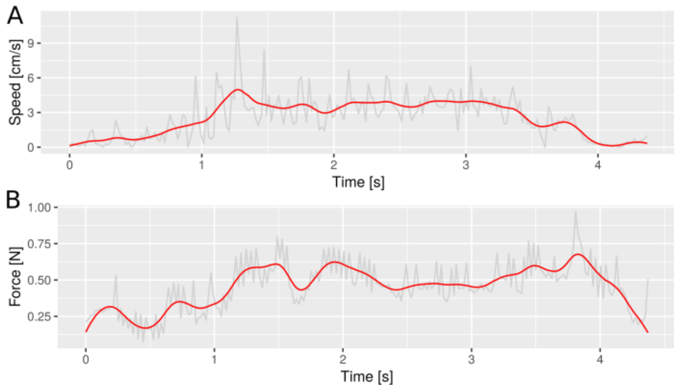


*Fig. S7. Velocity and Force profile in a representative participant. Raw data (light gray) and filtered data (red). (A) Velocity profile. (B) Force profile.*

Motion velocity was computed as follows. For each time interval, we measured the displacement of the finger on the XY plane as the Euclidean distance between two successive x and y positions. We computed the motion velocity as the ratio between the displacement in a give time-interval and duration of this interval. Fig. S8, S9, and S10show the distribution of peak velocities across trials and participants, in the three experiments. In Exp. 1, the median value was 7.2 $cm\ s^{-1}$ (95% percentile range from 4.0 to 19.0 $cm\ s^{-1}$). In Exp. 2, the median value was equal to 19.3 $cm\ s^{-1}$ (95% percentile range from 10.4 to 34.5 $cm\ s^{-1}$). In Exp. 3, the median value was equal to 25.4 $cm\ s^{-1}$ (95% percentile range from 11.8 to 45.4 $cm\ s^{-1}$). Participants did not receive any feedback about their motion velocity, and this may explain the variability between participants and between the three experiments. Despite the difference in peak velocity, the effect of ridge orientation on the angular error was comparable across the three experiments. Future experiments (for e.g. manipulating the velocity parametrically) are necessary to assess whether the angular error may change with peak velocity.

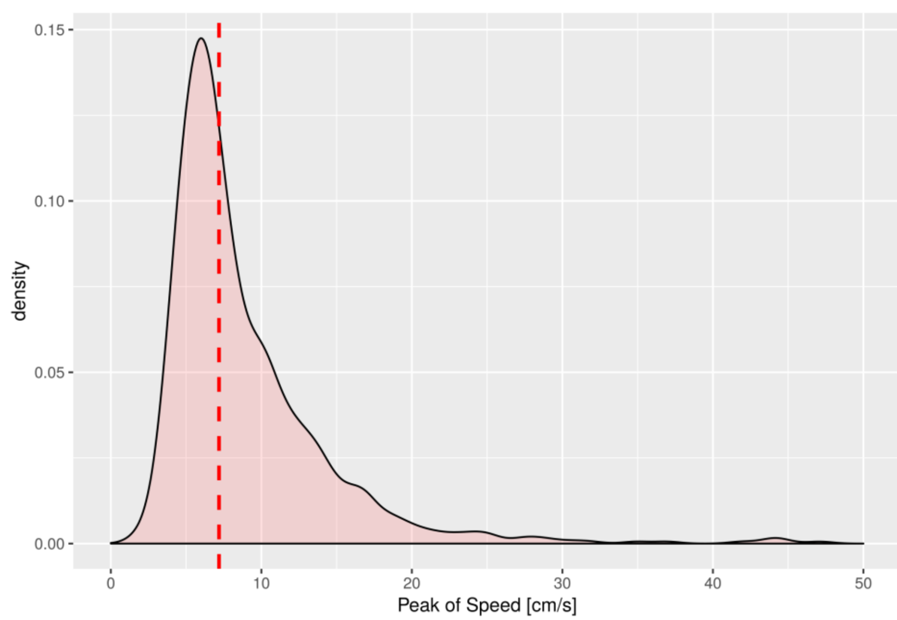


*Fig. S8. The distribution of peak velocity across trials and participants in Exp. 1. The dashed red line in the median value of peak velocity.*

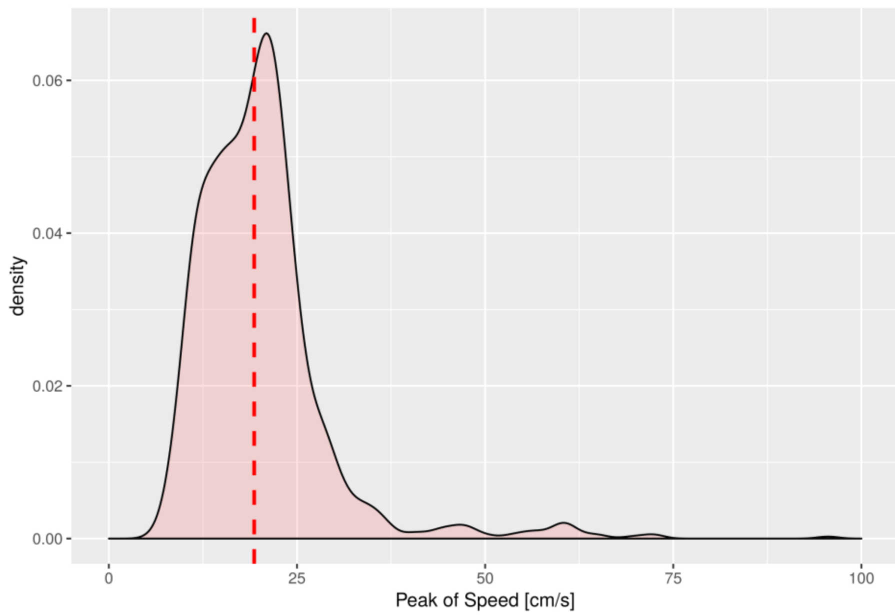


*Fig. S9. The distribution of peak velocity across trials and participants in Exp. 2 (Glove/No Glove Experiment).*

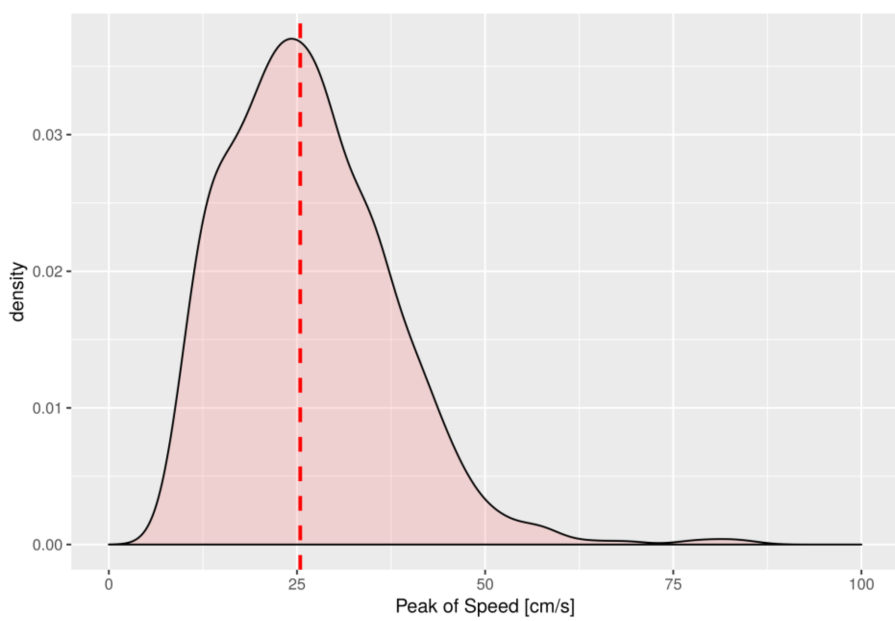


*Fig. S10. The distribution of peak velocity across trials and participants in Exp. 3 (Virtual Target Experiment)*

Next, we analyzed the distribution of the force peak and its relationship with the other experimental variables. In approximately 10% of the trials (mostly from participant 3 and 4) the load cell returned negative force values, possibly due to a drift in the calibration during the experimental session. Negative force values were discarded in the following analyses. In Exp. 1, the median value of peak force was 0.89 N (95% percentile range from 0.04 to 1.87 N). Using Linear Mixed Model (LMM), we related the force peak data to the ridge orientation. We interpolated the force peak data by means of a second order polynomial:

$$\mathbf{F} = \theta_0 + u_0 + \theta_1 \mathbf{X} + \theta_2 \mathbf{X}^2,$$

where **F** is the force peak, **X** is the orientation of the ridges, $u_0$ is the random intercept and $\theta_*$ the fixed effect parameters, respectively. Grating orientation had little effect on force peak. From LMM we estimated the average value of force peak for a perpendicular (zero) orientation of the stimulus and this was equal to $0.92 \pm 0.10$ N ($\theta_0 \pm$ SE). The difference in force peak between clockwise and counterclockwise ridges was small and equal to 0.08 N (peak at 60 deg counterclockwise minus peak at 60 deg clockwise) and 0.04 N (peak at 30 deg counterclockwise minus peak at 30 deg clockwise). Next, we investigated whether the motion bias related to the ridge orientation was modulated by the contact force, as follows. We fit the data with a multivariable LMM. The response variable was the motion angle and the two fixed-effect predictors were ridge orientation and average force, and the interaction of the two. This model confirmed a significant effect of ridge orientation ($\chi_1$ = 5.9, p = 0.016). Conversely, neither force ($\chi_1$ = 0.01, p = 0.9) nor the interaction term ($\chi_1$ = 2.1, p = 0.15) were statistically significant.

In Exp. 2, peak force was significantly larger in the with-glove condition compared with the bare fingertip condition ($p < 0.001$). The median value of peak force was equal to 0.84 N without glove and 1.0 N with glove. With glove, the average value of force peak for a perpendicular (zero) orientation of the stimulus was equal to $1.0 \pm 0.1$ N ($\theta_0 \pm$ SE), and decreased without glove (difference between conditions: $0.18 \pm 0.04$ N).

In Exp. 3, the average value of force peak for a perpendicular (zero) orientation of the stimulus and this was equal to $0.48 \pm 0.06$ N ($\theta_0 \pm$ SE), with negligible variations for grating orientation at $\pm 60$ deg.